Improved Ray Hierarchy Alias Free Shadows

Technical Report 2011:09
ISSN 1652-926X

Ola Olsson and Ulf Assarsson

May 6, 2011

Abstract

In this article, we introduce and evaluate several new algorithmic improvements to *Ray Hierarchies*. The improved algorithm is used to produce ray-traced shadows for omni-directional lights in fully dynamic environments. The new algorithmic improvements increase culling rate of the traversal algorithm, in some cases dramatically cutting the number of visited nodes. To evaluate performance, we present a GPU implementation using CUDA, which uses a hybrid breadth-depth algorithm to perform the traversal using bounded memory. The results show that the use of improved cone hierarchies is able to produce high quality shadows quickly – for some scenes in real-time.

1 Introduction

Shadows, it is well known, are very important for visual fidelity in computer generated images. The most popular algorithm for real-time shadows is shadow mapping, owing to its flexibility and high performance. This technique, while fast, suffers from various forms of aliasing [SD02] and are limited to a single plane of projection. It also requires storage for one or several high resolution shadow maps. Ray tracing, and equivalent techniques, solves the aliasing problems. However, they also generally require random access to the scene database and do not generally offer real-time performance for dynamic scenes.

In this paper we show how ray hierarchies can be improved and applied to bridge the gap between shadow mapping and ray tracers that use scene hierarchies. The new method extends cone hierarchies [RAH07] with several improvements for different scene types. This allows interactive or real-time ray traced (i.e. *alias free*) shadows for fully dynamic scenes. As the technique requires no hierarchy imposed on the scene data, it is simple to integrate into existing real-time renderers.

To improve the cone hierarchies we contribute a novel *precise cone/triangle intersection test*, and extend this to perform *early accept of covered cones*. We also introduce a two pass traversal, which exploits good blockers to speed traversal. Furthermore, we present a novel way to extract coherency by applying a sorting pass when screen space coherency is low, yielding much tighter cone hierarchies. We also contribute a *practical evaluation* on a number of scenes, demonstrating a *robust* GPU-implementation with bounded memory use.

2 Previous Work

Owing to the importance of shadows, there exists a vast corpus of previous work on shadow algorithms. Several good surveys on the topic provide a more comprehensive background than allowed by the scope of this article [WPF90, HLHS03, EASW09].

2.1 Shadow Map based methods

The most popular real-time (hard) shadow algorithm is *Shadow Mapping*, and derivatives thereof. The popularity stems from fast execution on GPUs, low requirements on scene data organization, and predictable rendering performance. The method suffers from several kinds of aliasing problems: projective, perspective and depth-precision aliasing [SD02].

Several approaches attempt to reduce aliasing through warping and/or partitioning [LTYM06]. These approaches are generally real-time, but suffer from special cases which makes them difficult to use in interactive applications.

Partitioning is taken further with *Resolution Matched Shadow Maps* [LSO07], which manage a virtual shadow map of very high resolution. Only the pages required for the current view are allocated and rendered, at the required resolution. Perspective and projective aliasing is much reduced, but not eliminated. The implementation achieves real-time performance for moderately large scenes, but is quite complicated to implement efficiently.

All shadow map techniques need a plane of projection, and therefore need several rendering passes and shadow maps, to support omni-directional lights, e.g. a cube map or some other partitioning [For04, LTYM06]. In this paper we present a ray tracing based solution that does not have this limitation, and avoids all types of aliasing except depth-precision. The new method also shares the advantage of low requirements on scene data organization, with shadow mapping.

2.2 Ray Tracing based methods

Ray tracing solves the hard shadow problem exactly, and thus does not suffer from the aliasing resulting from discretization (perspective, and projective aliasing). General ray tracing can handle any type of light. However, general ray tracing methods generally require random access to the scene database, and a highly optimized scene hierarchy.

There are now several publications showing real-time, or interactive, performance for ray traced solutions of small to moderate scene sizes. The most recent both construct acceleration structures and trace rays on the GPU [ZHWG08, LGS$^+$09].

Alias free shadow maps [AL04], variations and implementations [JLBM05, Arv07, SEA08], compute an equivalent result to ray traced solutions by performing irregular rasterization. The most recent work offer interactive performance [SEA08], but requires special geometry. All of these methods need a plane of projection, and consequently, do not support omni-directional light sources.

Cone hierarchies that exploit screen space coherency for fast ray hierarchy construction on the GPU have been demonstrated [RAH07]. They offer real-time, or interactive, performance for scenes with high screen space coherency. However, the previous work does not specifically explore shadows, but instead the discussion centers on solving specular and glossy phenomena. In this work, we improve this algorithm and tailor it to the problem of shadows. We also introduce a sorting pass, based on space filling curves, to improve coherency when there are discontinuities in image space.

3 Improved Cone Hierarchy Traversal

The approach taken in this paper is an extension of the *Ray-Space Hierarchy* algorithm presented by Roger et al [RAH07]. As noted in their paper, the bottom up construction used produces inefficient bounding volume hierarchies when there are incoherent rays near the bottom of the tree. This is because cones become large if the angle between the rays is large, and these cones then propagate up the bounding volume hierarchy.

Incoherent rays are especially common when tracing reflections and refractions through several bounces. We instead focus on the problem of shadows, where significant image space coherency can be expected, for *interesting scenes* [LSO07]. The coherency exists because all the shadow rays share one common endpoint, the light; and because nearby samples usually are located close together in world space.

By focusing on shadows, we can also exploit some special properties of shadow rays to construct an improved traversal algorithm. Shadow rays are, for example, finite and all share one endpoint (the light).

However, solely using screen space coherency is not sufficient for constructing efficient ray hierarchies. Discontinuities in the depth buffer can cause large cones near the bottom of the tree. To address these situations we also propose some novel techniques for improving coherency before constructing cone trees.

3.1 Algorithm Overview

The basic algorithm consists of the following steps, and follows, more or less the approach in previous work [RAH07].

1. Rasterize the scene, but store the direct light contribution in a separate render target (light buffer).
2. Construct a ray hierarchy using the Z buffer and light buffer.
3. Intersect the scene geometry with the ray hierarchy.
4. Set all pixels that correspond to a ray/triangle intersection to black in the light buffer.
5. Add the light buffer to the frame buffer.

In the first step, the scene is rasterized as per normal, and lighting is computed for the samples. However, instead of adding the direct light component, this is stored in a texture, such that it can be added later after shadowing has been computed. Naturally, it is equally possible to perform a depth only pass first, then compute shadows, and finally compute shading only where necessary.

Next, the ray hierarchy is constructed in a way similar to a mip-map hierarchy. Starting from individual rays (which are reconstructed from the z buffer and light position), a four-way bounding volume tree of cones is constructed [RAH07]. Note that each leaf location corresponds directly to a sample in the light buffer.

To find which samples are shadowed, each triangle is used to traverse the ray hierarchy from the root. The traversal step is performed using breadth first traversal. When all the internal levels in the hierarchy have been traversed, we have a list of ray/triangle pairs. The ray/triangle pairs are tested for intersection, and if found, the corresponding light buffer sample is set to black.

Finally the light buffer is simply added, fragment by fragment, to the frame buffer, producing a correctly lit and shadowed scene.

3.2 Precise Cone/Triangle Intersection

The previous work [RAH07], uses bounding spheres around the primitives when traversing the hierarchy. A bounding sphere quite severely overestimates the volume of a triangle, and thus inflates the probability of intersection with a cone or a ray. This leads to many nodes being traversed needlessly, which is especially problematic for large triangles, for example walls of buildings, Figure 1 illustrates this problem.

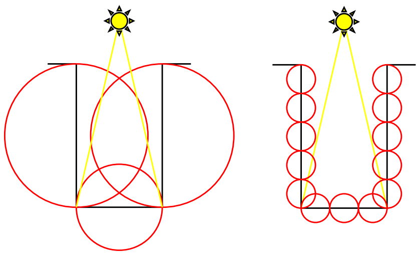

Figure 1: *Bounding spheres provide severely over-conservative bounds on triangles, especially long and skinny triangles. The illustration shows a schematic view of a city street, with tall walls. In the left version, bounding spheres (red) interact with* every *ray inside the cone (yellow), though none actually intersect the wall. To the right, the scene has been subdivided, which reduces the problem, but at the cost of several times more primitives.*

A simple way to attempt to address this problem is to subdivide the scene triangles (Figure 1 right). However, the tessellation would have to be adaptive to handle different views, and trades simplicity in intersection for more open traversal nodes.

To better address this problem we instead introduce a more precise cone/triangle intersection test. The new test is based on homogeneous triangle rasterization, and starts by constructing a perspective projection from the cone. Then, the triangle vertices are transformed into the cones homogeneous clip space, and the homogeneous edge equations are constructed from the transformed vertices [AMMH07]. If the signed distance from *any* edge to the origin is greater than one, the triangle can be rejected, see Figure 2(a). The signed distance to the origin is trivially obtained from the edge equations by normalizing them. Figure 2(b) shows an example which cannot be rejected, as none of the signed distances are greater than one (d_1 and d_2 are negative while d_0 is positive but smaller still than one).

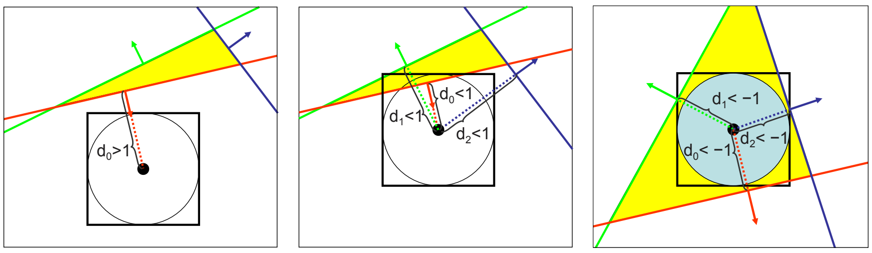

(a) Rejected triangle. (b) Intersected triangle. (c) Accepted triangle.

Figure 2: *The triangle is transformed using the cone projection, and the edge equation distances compared against the unit circle.*

We also determine the nearest point on the intersection between the cone and triangle supporting plane, illustrated in Figures 3(b) and 3(c). The distance to this point is used to determine if the cone hits the triangle plane at all: if it is larger than the longest ray represented, L_{max} (Figure 3(a)), then the cone cannot intersect the triangle. This test is implemented by exploiting calculations performed during projection. We set the far plane distance of the cone projection to L_{max}, and align the up direction of the projection with the normal of the triangle. After projection, the homogeneous triangle plane equation is formed, and then solved for Z_{near} at the homogeneous point $P_{near} = \{0, -1, Z_{near}, 1\}$. Because of the way we chose the far clip distance, the cone can be rejected if $Z_{near} > 1$.

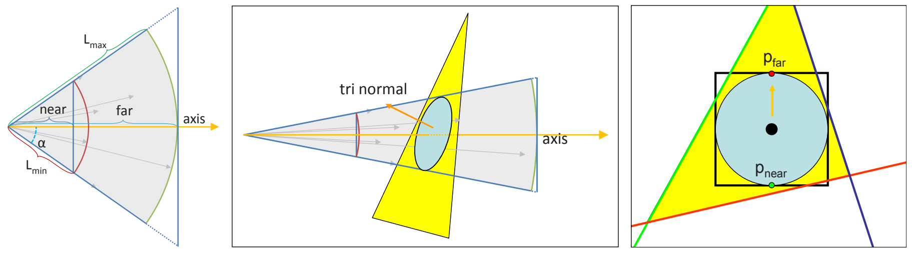

(a) Cone properties. (b) A covered cone, with triangle normal. (c) The clip space up direction is aligned with the triangle normal.

Figure 3: *Note, in (a), that the cone angle α is the half spread angle and has a valid range of $[0, \pi]$. Shown in gray are some example rays represented by the cone, with their shortest and longest lengths, L_{min} and L_{max}, indicated. In (c), the clip space locations of P_{near} and P_{far} are shown.*

A problem with the new test is what is sometimes termed the triangle shadow (see Figure 4. The triangle shadow is the area outside the triangle where none of the edge distances are less than one. Such triangles are therefore incorrectly classified as intersecting. This leads to more nodes than necessary being traversed and can actually lead to worse culling performance than the sphere test if left unchecked. To solve this we also construct and test separating planes tangential to the unit circle with the normals pointing towards the vertices. If all three vertices are outside any of these planes, the triangle is rejected.

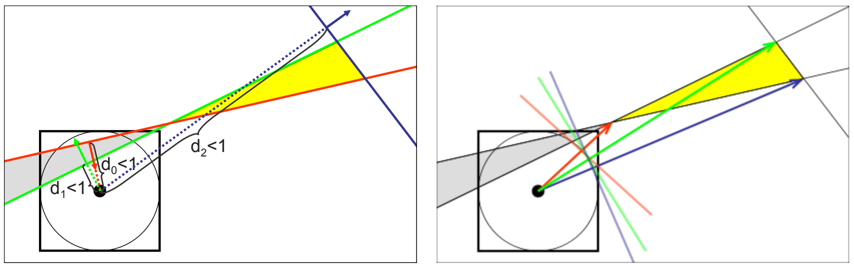

(a) The triangle shadow. (b) Triangle shadow solution.

Figure 4: *The triangle shadow is the area outside the triangle, but where no plane distance is greater than one (a). Our solution, (b), a separating plane is found between each vertex and the unit circle, and if all vertices are outside any of these, then the triangle is rejected.*

For cone angles near and above $\pi/2$ the projection becomes unstable. Therefore, if the angle is greater than $\pi/2 - \varepsilon$, using some small machine dependent epsilon ε, the angle is rounded up to $\pi/2$. For these large angles, the test is changed to check if all vertices are contained in the complementary cone: if all three points are inside the complementary cone, then there is no intersection.

3.3 Early accept for covered cones

The new test uses the exact representation of the scene geometry, as opposed to conservative bounds. This means that it is now possible to construct a test that determines if the cone is completely covered by the triangle. Extending the homogeneous test, the triangle covers the cone if all the distances to the edges are less than the negative one, see Figure 2(c).

To correctly determine if all the rays represented by the cone has intersected the covering triangle, one new piece of information is needed: the length of the *shortest* of these rays, L_{min}. Adding this information is a trivial addition to the tree construction algorithm. We can then assert whether the farthest point on the intersection between the cone and the triangle lies closer than the length of the shortest ray. If this is the case, all the rays must cross the triangle plane, and therefore intersect the triangle. For infinite rays, this last check can be omitted, as the rays must intersect any triangle covering the cone.

To determine the nearest crossing, we re-use the logic used to find the nearest crossing point (see Section 3.2). After constructing the clip space triangle plane, we solve for Z_{far} at the homogeneous point $P_{far} = \{0, 1, Z_{far}, 1\}$, see Figure 3(c). When constructing the cone projection, the near clip distance is set to $L_{min} \cos \alpha$, which is necessary since we must allow for the fact that the shortest ray may diverge from the cone axis by the cone angle (see Figure 3(a) for an illustration). Because of this choice of near plane, if $Z_{far} < -1$, then all rays must hit the triangle.

When a cone is found to be completely covered, we can simply set all the corresponding fragments to "shadowed", and remove the element from the traversal queue. As the cone tree is left-balanced and implicit, it is trivial to find the corresponding range of leaves from any interior node.

Furthermore, since this cone has been identified as covered, we know that it is not necessary to test any more primitives against it nor any of its children. Thus we can mark the node in the tree as invalid. As traversal is breadth first we can in the next pass test each element to see if the parent node is valid, and terminate traversal if not (see Figure 5).

3.4 Two-Pass traversal

Testing the coverage of triangles helps pruning many branches of the traversal tree. However, a cone may be covered not by one, but by two or more triangles each covering only part of the cone. This situation occurs along all interior edges when occluders consist of more than one triangle, and cannot be detected by the early accept test.

To address this, a variation is introduced that traverses the triangles in two passes. In the first pass, only those triangles that are good candidates for occlusion are traversed through the ray hierarchy. After this, if the selected blockers were indeed good, large portions of the light buffer should be marked as shadowed. Next, the hierarchy is updated, removing those rays that are already in shadow. Finally, all remaining triangles are traversed using the new smaller cone hierarchy.

It is not immediately obvious what makes a good occluder, but for architectural scenes, large walls are good candidates. If the first pass does not produce many finished

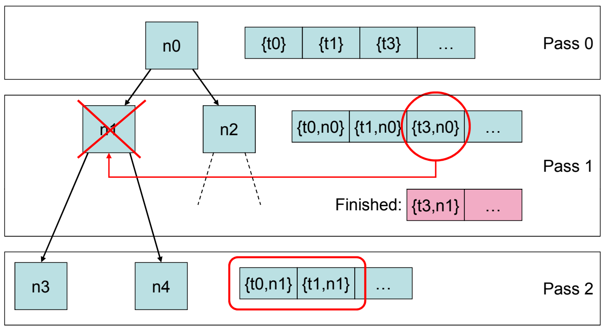

Figure 5: *In pass 0, all triangles are tested against the root node; those that pass are added to the traversal queue. In pass 1, the children of the queued nodes are tested; those that pass are added to the queue for the next level, and those that cover the cone are marked as finished. In the example, t3 covers the cone in node n1. As a side effect, the corresponding node is marked as invalid. In pass 2, then, the parent nodes are checked for validity. The circled nodes are thus trivially terminated.*

rays, the update step can be skipped, and thus the only time lost is due to the overhead of launching kernels and potentially under-utilizing the GPU if there are not enough large polygons in the first batch. For very large scenes, this overhead is minor. For some scenes, it may also be beneficial to place occluders manually or automatically generate them from the scene data.

3.5 Ray Sorting

The naive approach to constructing cone hierarchies from the frame buffer assumes that the rays are already coherent. While this is a reasonable assumption for shadow rays shot from continuous surfaces, it starts to break down where there are depth discontinuities. An example of a problematic situation is shown in Table 2. However, while pixels are not directly coherent in screen space, they are still so in *world space* as they originate from locations nearby each other. Introducing a ray sorting pass before hierarchy construction is an attempt to extract this coherency in order to improve cone tree quality.

Before sorting the rays a compaction step is performed to remove any rays from pixels that are not affected by the light. Compaction is very cheap, especially compared to sorting. Next, a sorting key based on a space filling curve is constructed for remaining sample. We use a method inspired by what was presented in [AK87], partitioning the direction space into six square 2D spaces, according to the ray direction major axis coordinate. Within each of the 2D spaces, the ray direction is represented by the two remaining coordinates, normalized to the range $[-1,1]$. From this 2D coordinate, we find the number on a discrete Hilbert curve, with a resolution selected to efficiently use the bits in the 32-bit sorting key. The rays are then sorted according to these keys using a fast radix sort. After sorting using of the Hilbert order, rays with similar directions should be close together.

The construction stage is also modified slightly. Since the rays are no longer stored in a 2D grid (i.e. screen space), but in an 1D vector, we build the tree four consecutive elements at a time. We retain the use of four-way trees as these offer a good trade-off between bandwidth use, memory use and number of passes required. Note that we still construct a left-balanced implicit tree, as opposed to attempting to construct the hierarchy directly from the keys [LGS+09]. Retaining this tree layout means that it is still easy to find the range of leaves that correspond to an internal node, which we exploit for the early accept.

3.6 Front face Culling

It it common to avoid the problem of self shadowing due to limited depth precision by applying front face culling. I.e., the shadow casting geometry only consist of the light back facing triangles, and only these are tested against the ray hierarchy. This assumes that the front face culled geometry is two-manifold (closed).

We apply this technique, but also for performance reasons. By culling the triangles from which the shadow rays originate, we can quickly reject triangles that would otherwise have to traverse all the way to the leaves, but not contribute any shadow. The culling test uses the angle between the cone and triangle normal.

4 Experimental Evaluation

The rasterization was implemented using OpenGL and the ray tracing steps using CUDA [NVI08]. The depth and light buffers were mapped into CUDA address space and accessed as linear memory buffers. We implemented the original approach using spheres and added the improvements described in the previous sections.

4.1 Implementation Details

For the compaction step used in the breadth first traversal, we use the algorithm described in [BOA09], available in the `chag::pp` library. This design is about an order of magnitude faster than what was used in previous work [RAH07], thus removing compaction as a major bottle neck.

To intersect rays and triangles, we use the test described by Wald [Wal04], adapted to suit current GPU capabilities. This test relies on pre-computation of the triangle properties, which roughly doubles storage required for triangles. For situations where scene geometry storage is important, the Möller-Trumbore test [MT05] may be more appropriate.

4.2 Bounded Breadth First Traversal

In the previous work on cone hierarchies, there were problems with breadth first traversal overflowing. This happens for large scenes, or where primitives overlap many nodes (due to poor coherency, for example). We solve this by using a hybrid traversal scheme. A fixed size separate buffer is allocated on the GPU for each pass. Recursion is then used to completely traverse a sub-set of the input whenever the output from the current pass would overflow the next buffer.

This keeps the beneficial properties of breadth first traversal, ensuring high utilization of computational units. We also achieve a fixed bound on memory use, like depth first traversal.

4.3 Efficient Data Representation

The general cone hierarchy representation stores a cone and a sphere for each node, using 8 floating point numbers. By treating the rays as if they are cast from the light source we get a common origin for all the cones, which allows us to halve the storage required for the hierarchy by leaving the spheres out. This speeds up both traversal and construction, and also yields a hierarchy of tight cones ending in a point.

For rays, one endpoint can be reconstructed from the depth buffer, and the other is represented by the light source. This means no extra buffers are required for rays, which represents a substantial saving in bandwidth and storage.

5 Results and Discussion

The algorithm was tested on the following animated scenes: the BART robots scene, with 71706 triangles [LAM01]; and the BART museum scene at maximum tessellation, 75948 triangles. To evaluate the impact of each improvement, we implemented several combinations, listed in Table 1. All performance measures were carried out using an NVIDIA GTX580 GPU and rendered at a screen resolution of 1024x1024.

Table 1: *The evaluated algorithm variations, and their short hands used in the text.*

	Cone/Triangle Test	Sorting	Early Accept	Two-Pass
Precise	Precise	No	No	No
PreciseSorted	Precise	Yes	No	No
Spheres	Sphere	No	No	No
SpheresSorted	Sphere	Yes	No	No
PreciseSEA	Precise	Yes	Yes	No
PreciseEATP	Precise	No	Yes	Yes
PreciseSEATP	Precise	Yes	Yes	Yes

In Figure 6, we show results from the robots scene for bounding spheres and precise triangle test, both with and without sorting, to evaluate the impact of sorting. It can be seen that the methods based on sorting always visit fewer nodes than those that are based on screen space coherency alone (Figure 6(a)). Around frame 100 (shown in Figure 6(c)), there is a distinct gap between sorted and unsorted methods, owing to the lack of screen space coherency caused by the camera looking down the corridor but with some robots in the foreground. It is also clear that the variants using the precise triangle test always visit fewer nodes than the bounding sphere variants.

The robot scene has some very large triangles in the buildings, which largely align with the light direction. This favors the precise triangle test, which consequently visits much fewer nodes, as can be seen in Figure 6(a). This is especially pronounced around frame 160, where the camera is pointing almost directly at a wall. Consequently, the rays are both highly coherent and also graze the triangles in the wall. The precise methods need only process a couple of hundred nodes in this case, whereas both sphere based methods must visit close to 50 million nodes. Also worth noting around frame 160 is that because of already high screen-space coherency, it shows the same number of nodes processed regardless of whether sorting is utilized.

When considering run-time performance (Figure 6(b)), the ranking of the methods is no longer quite as clear. The precise intersection test is more expensive than the

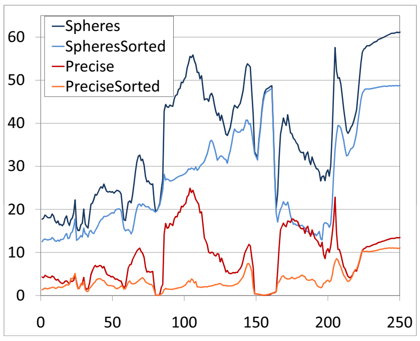

(a) Millions of nodes processed.

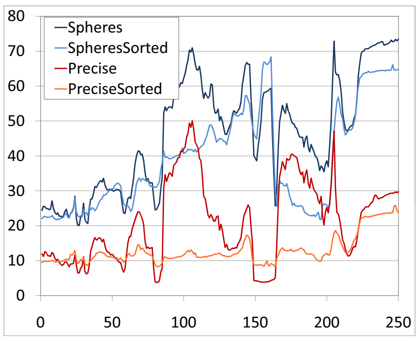

(b) Milliseconds to compute shadow.

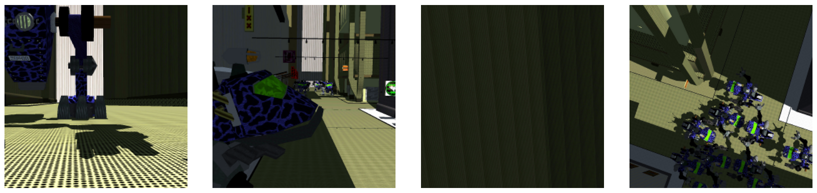

(c) Thumbnails from animation, frames 20, 105, 160 and 243.

Figure 6: *Measurements from the animation in the BART robots scene, comparing the impact of sorting on the basic sphere based method and when using the precise cone triangle test. (a) shows the number of nodes traversed, and (b) shows the shadow computation time. In (c), are screen shots from the animation showing . Note that frame 160 shows the camera pointing straight at the wall.*

simpler sphere test, which means that when equal number of nodes are traversed the simpler test wins. Furthermore, the sorting imposes a fairly constant overhead (around four milliseconds). The most clear trend is that the precise test with sorting is the best performing variant, except in those circumstances where the screen space coherency is already high. The precise test with soring also offers the least variable performance, which is an important feature for real-time applications.

Figure 7 details performance figures using early accept and the two-pass approach. We show graphs for the sorted varieties only, and using the precise triangle test, as the differences are similar for the other variations. Notice that the number of nodes culled is steadily improved with each new optimization, but that the time to compute shadow is almost the reverse. This is because of the more complicated test, but also because that the compaction step in the breadth first traversal must be replaced with a more expensive split operation, which is needed to filter out the elements that are finished.

To further investigate the effect of screen space coherency, we used the museum scene, see Table 2. This scene contains a large quantity of small triangles that are independently animated.

For this scene, contrary to what we saw for the robots scene (Figure 6), the unsorted spheres method often offers better performance than the unsorted precise triangle method. This is because the majority of the shadow casters are very small, which means that they reasonably well approximated by bounding spheres (see Section 3.2). The precise version still prunes more nodes, but not sufficiently to compensate for the more expensive precise triangle test. When sorting is used, however, the performance gap increases, and the precise method is faster in all views. This shows that the pre-

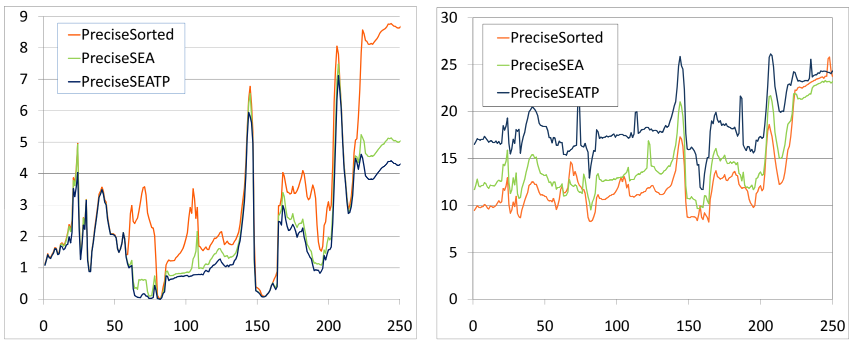

(a) Millions of nodes processed. (b) Milliseconds to compute shadow.

Figure 7: *Measurements from the robot scene animation, showing the impact of enabling early accept and two pass processing.*

cise culling test interacts favorably with the tighter cone tree produced by the sorting method.

Notably, for the third view in Table 2, the sorting only improves the quality of the resulting tree slightly. This view exhibits very high screen space coherency, and can therefore not be improved much by sorting. That the shadowing performance is lower in this case is not surprising, given that there is a cost for sorting the rays.

6 Conclusion

We have shown that the improved cone hierarchies are capable of producing real-time shadows on modern GPUs. The new algorithm provides improved pruning of the traversal tree and the tree quality, when compared to previous approaches. The more precise triangle test has a large impact on culling performance in most scenes, demonstrating that spheres are indeed poor bounding volumes for large triangles. Scenes with a larger proportion of small triangles (such as the museum scene) does not benefit as much from this improvement.

The early accept and two-pass approach improve traversal pruning even further. However, due to the increased cost for each node, do not yield any run time performance advantage on current GPUs.

The application of sorting yields an enormous improvement for scenes with low screen space coherency, especially when combined with the precise test. The results show up to three orders of magnitude fewer nodes traversed, and over two orders of magnitude faster shadow computation.

Another important performance aspect is variability. Low variability is desirable, especially for real-time applications such as games that need to maintain a smooth frame rate. The precise test combined with sorting enables less variable frame times. The early accept also has the potential to help with this, as the problematic case of a triangle close to the light (which would traverse all paths), is turned into an advantage. However, this effect is not apparent is the test results.

Table 2: *BART Museum scene, comparing sorted and unsorted performance for the basic sphere intersection variant and precise triangle variant, on a set of views with varying screen space coherency.*

	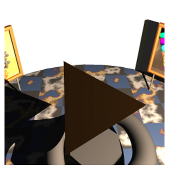	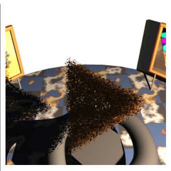	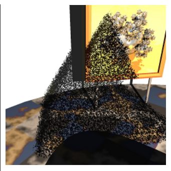	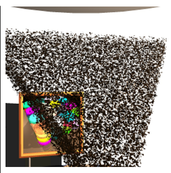
	Shadow compute time (ms)			
Spheres	29.40	446.10	10.53	3771.55
SpheresSorted	11.90	16.75	15.05	16.69
Precise	38.50	557.91	8.26	4172.61
PreciseSorted	10.65	13.40	12.63	12.60
	Number of nodes			
Spheres	19.89M	317.91M	5.77M	2199.22M
SpheresSorted	2.66M	6.79M	5.40M	6.60M
Precise	17.58M	292.84M	2.25M	2163.30M
PreciseSorted	0.82M	2.24M	2.20M	1.97M

7 Future Work

In the future, the sorting and improved cone tree traversal should be applied to general ray tracing, as most of the techniques introduced are applicable for rays other than shadow rays. For this to be successful there are several important challenges, for example adapting the sorting to handle rays with disparate endpoints.

Ray hierarchies are very closely related to the problem of constructing ray packets, for packet based scene hierarchy traversal. Thus, an interesting future direction is to combine the efficient cone tree construction with a more conventional packet based GPU ray tracer. By traversing these truly hierarchical packets, and employing the early accept test, very high performance should be possible.

References

[AK87] James Arvo and David Kirk. Fast ray tracing by ray classification. *SIGGRAPH Comput. Graph.*, 21(4):55–64, 1987.

[AL04] Timo Aila and Samuli Laine. Alias-free shadow maps. In *Proceedings of Eurographics Symposium on Rendering 2004*, pages 161–166. Eurographics Association, 2004.

[AMMH07] Tomas Akenine-Möller, Jacob Munkberg, and Jon Hasselgren. Stochastic rasterization using time-continuous triangles. In *Proceedings of the 22nd ACM SIGGRAPH/EUROGRAPHICS symposium on Graphics hardware*, pages 7–16, Aire-la-Ville, Switzerland, Switzerland, 2007. Eurographics Association.

[Arv07] Jukka Arvo. Alias-free shadow maps using graphics hardware. *journal of graphics, gpu, and game tools*, 12(1):47–59, 2007.

[BOA09] Markus Billeter, Ola Olsson, and Ulf Assarsson. Efficient stream compaction on wide simd many-core architectures. In *HPG '09: Proceedings of the Conference on High Performance Graphics 2009*, pages 159–166, New York, NY, USA, 2009. ACM.

[EASW09] Elmar Eisemann, Ulf Assarsson, Michael Schwarz, and Michael Wimmer. Casting shadows in real time. In *ACM SIGGRAPH ASIA 2009 Courses*, SIGGRAPH ASIA '09, New York, NY, USA, 2009. ACM.

[For04] Tom Forsyth. Practical shadows. Game Developers Conference, 2004. `http://home.comcast.net/~tom_forsyth/papers/papers.html`.

[HLHS03] Jean-Marc Hasenfratz, Marc Lapierre, Nicolas Holzschuch, and François Sillion. A survey of real-time soft shadows algorithms. *Computer Graphics Forum*, 22(4):753–774, dec 2003.

[JLBM05] Gregory S. Johnson, Juhyun Lee, Christopher A. Burns, and William R. Mark. The irregular z-buffer: Hardware acceleration for irregular data structures. *ACM Trans. Graph.*, 24:1462–1482, October 2005.

[LAM01] Jonas Lext, Ulf Assarsson, and Tomas Möller. A benchmark for animated ray tracing. *IEEE Comput. Graph. Appl.*, 21:22–31, March 2001.

[LGS$^+$09] Christian Lauterbach, Michael Garland, Shubhabrata Sengupta, David Luebke, and Dinesh Manocha. Fast bvh construction on gpus. *Comput. Graph. Forum*, 28(2):375–384, 2009.

[LSO07] Aaron E. Lefohn, Shubhabrata Sengupta, and John D. Owens. Resolution-matched shadow maps. *ACM Trans. Graph.*, 26(4):20, 2007.

[LTYM06] D. Brandon Lloyd, David Tuft, Sung-Eui Yoon, and Dinesh Manocha. Warping and partitioning for low error shadow maps. In Tomas Akenine-Möller and Wolfgang Heidrich, editors, *Proceedings of the Eurographics Workshop/Symposium on Rendering, EGSR*, pages 215–226, Aire-la-Ville, Switzerland, June 2006. Eurographics Association.

[MT05] Tomas Möller and Ben Trumbore. Fast, minimum storage ray/triangle intersection. In *SIGGRAPH '05: ACM SIGGRAPH 2005 Courses*, page 7, New York, NY, USA, 2005. ACM.

[NVI08] NVIDIA. Cuda zone: Toolkit & sdk, 2008.

[RAH07] David Roger, Ulf Assarsson, and Nicolas Holzschuch. Whitted ray-tracing for dynamic scenes using a ray-space hierarchy on the gpu. In Jan Kautz and Sumanta Pattanaik, editors, *Rendering Techniques 2007 (Proceedings of the Eurographics Symposium on Rendering)*, pages 99–110. Eurographics and ACM/SIGGRAPH, the Eurographics Association, jun 2007.

[SD02] Marc Stamminger and George Drettakis. Perspective shadow maps. In John Hughes, editor, *Proceedings of ACM SIGGRAPH*, Annual Conference Series, pages 557 – 562. ACM Press/ ACM SIGGRAPH, July 2002.

[SEA08] Erik Sintorn, Elmar Eisemann, and Ulf Assarsson. Sample-based visibility for soft shadows using alias-free shadow maps. *Computer Graphics Forum (Proceedings of the Eurographics Symposium on Rendering 2008)*, 27(4):1285–1292, June 2008.

[Wal04] Ingo Wald. *Realtime Ray Tracing and Interactive Global Illumination*. PhD thesis, Computer Graphics Group, Saarland University, 2004.

[WPF90] Andrew Woo, Pierre Poulin, and Alain Fournier. A survey of shadow algorithms. *IEEE Comput. Graph. Appl.*, 10(6):13–32, 1990.

[ZHWG08] Kun Zhou, Qiming Hou, Rui Wang, and Baining Guo. Real-time kd-tree construction on graphics hardware. *ACM Trans. Graph.*, 27(5):1–11, 2008.